Top Organomet Chem (2010) 28: 57–73
DOI: 10.1007/978-3-642-01866-4_2

NLO Molecules and Materials Based on Organometallics: Cubic NLO Properties

Mark G. Humphrey, Marie P. Cifuentes, and Marek Samoc

Abstract Relevant background theory, experimental procedures, and significant recent advances in the third-order NLO properties of organometallic complexes are reviewed, with particular emphasis on spectral dependence studies and switching of nonlinearity.

Keywords Cubic nonlinearity, Molecular switches, Nonlinear absorption, Nonlinear refraction

Contents

M.G. Humphrey (✉) and M.P. Cifuentes
Research School of Chemistry, Australian National University, Canberra, ACT 0200, Australia
e-mail: Mark.Humphrey@anu.edu.au, Marie.Cifuentes@anu.edu.au

M. Samoc
Institute of Physical and Theoretical Chemistry, Wroclaw University of Technology, 50–370 Wroclaw, Poland
e-mail: Marek.Samoc@pwr.wroc.pl

1 Introduction

Nonlinear optical (NLO) effects originate from high-intensity electric fields (such as those from laser beams) interacting with matter. These interactions can result in the electromagnetic field components of the incident light beam being modified, and new components (differing in phase, frequency, etc.) being generated. These effects can have a range of applications in laser technologies, optical signal processing, multiphoton information storage and retrieval, microscopy, and multiphoton photodynamic therapy, for example.

It can be challenging to meet the demands on prospective materials for device applications. Apart from the obvious requirement that NLO responses be sufficient for the specific application, the material needs to tolerate the device manufacturing and operating conditions (e.g., it needs to possess a sufficiently high damage threshold), as well as having acceptable photochemical and thermal stability or fluorescence efficiency (depending on the application). While crystals of inorganic salts and glasses currently dominate the market for second- and third-order NLO applications, respectively, there are shortcomings with aspects of their performance that have focused attention on organics and, more recently, organometallics as potential NLO materials. In particular, organometallics have the potential to combine the advantages of organics (such as fast response, ease of processing, and considerable design flexibility) with the benefits that may flow from incorporation of a metal center (such as variable oxidation state and coordination geometry).

In contrast to second-order nonlinearities, for which considerable success defining structure-property relationships has been achieved, considerably less is known of how to optimize third-order effects. Third-order optical nonlinearities of organometallic complexes were first reported in the mid-1980s. The promising early studies stimulated considerable interest, and an ever-increasing number of reports, the results from which have been summarized in several reviews that also include introductions to the background theory of nonlinear optics [1–8]. This chapter includes a brief overview of theory relevant to cubic NLO and a summary of experimental procedures to measure cubic nonlinearities, followed by a brief review highlighting the significant advances in the field over the past few years; while theoretical studies of the NLO properties of organometallics have attracted interest [9, 10], the emphasis here is on experimental outcomes.

2 Theory and Experiment in Third-Order NLO of Organometallics

2.1 Theory of Third-Order NLO Effects

When a molecule is exposed to an electromagnetic field, it is usually the electric component of the field that is of much greater significance than the magnetic component, and the response of the molecule is usually treated within a dipolar

approximation in which the whole interaction is described as the time evolution of a point dipole. Both of these approximations have limited value; for example, neglecting the magnetic interactions does not allow for the description of chirooptic effects, and assuming a point character of the dipole and neglecting the multipolar character of the effects may be inappropriate for large molecules such as dendrimers. However, the traditional approach to explaining the origin of NLO effects on the molecular scale is by simply assuming that an electric field of magnitude E creates a point dipole μ in a molecule, and this dipole can be expanded in series against the powers of E. Because μ and E are vectors, the equation relating them must take into account dependences of all of the Cartesian components of both vectors. Using Einstein's convention of summing over repeated indices and employing the esu system of units, one can write[1]:

$$\mu_i = \mu_i(0) + \alpha_{ij}E_j + \beta_{ijk}E_jE_k + \gamma_{ijkl}E_jE_kE_l + \ldots, \tag{1}$$

where μ_i are components of the total dipole moment, $\mu_i(0)$ is the dipole moment at low field strengths (the permanent dipole moment), α_{ij} is the molecular polarizability, β_{ijk} is the first hyperpolarizability (also called the second-order or quadratic polarizability), and γ_{ijkl} is the second hyperpolarizability (also called the third-order or cubic polarizability)[2]. The order of expansion in Eq. (1) determines the naming of the effects that are due to the consecutive terms: linear optical effects are those that are described by the linear polarizability α, quadratic NLO effects are due to β, and cubic NLO effects to γ.

Strictly speaking, Eq. (1) is only valid for static electric fields. For any field that is time dependent, i.e., $E(t)$, the molecular response $\mu(t)$ will always lag behind somewhat. This is taken into account by assuming that α, β, and γ are complex quantities, and that they relate Fourier components of the time-varying dipole moment to Fourier components of the time-varying electric field. In effect, Eq. (1) needs to be rewritten for the combination of field amplitudes and field frequencies that are of interest. Limiting the following to cubic NLO effects, such an equation will have the following form:

$$\mu_i^{(3)}(\omega_4) = \gamma_{ijkl}(\omega_4; \omega_1, \omega_2, \omega_3)E_j(\omega_1)E_k(\omega_2)E_l(\omega_3), \tag{2}$$

where an interaction of three fields at three frequencies ω_1, ω_2, and ω_3 leads to an induced nonlinear component of a dipole oscillating at $\omega_4 = \omega_1 + \omega_2 + \omega_3$.

[1]Note that the equations describing nonlinear optical effects can have different forms depending on the system of units used (esu or SI), the inclusion of the $1/n!$ factors of the power expansion in the coefficients or using them in front of the coefficients, and inclusion (or not) of the degeneracy factors that may appear in the equations, depending on the number of identical fields in a given nonlinear interaction. See, for example, [11].

[2]Note that some authors refer to β as the *first-order hyperpolarizability* and γ as the *second-order hyperpolarizability*. While this is formally correct, in the opinion of the present authors such nomenclature should be avoided since it can lead to confusion as to the order of the nonlinear process that is being described.

It should be noted that γ is a tensor with four indices, and thus has 81 components; the values of these components can depend on any of the frequencies in Eq. (2). Fortunately, symmetry considerations can reduce the number of independent tensor components considerably. In addition, the dispersion of γ can sometimes be simplified when specific NLO interactions are considered.

Cubic NLO processes can be termed *four-wave mixing* processes, because in each case described by Eq. (2), one deals with three input fields and an output field (oscillating at ω_4), the latter being generated by the nonlinear component of the induced dipole moment. Among the examples of wave mixing that are of practical importance, the simplest one occurs when only a single frequency field originating from a single light beam is present. In this case, the field is described by:

$$E(t) = \frac{1}{2}E(\omega)[\exp(-\mathrm{i}\omega t) + \exp(\mathrm{i}\omega t)] \tag{3}$$

and the cubic nonlinear interaction has only two forms: either the frequencies of the three amplitudes in Eq. (2) sum to form the third-harmonic of the fundamental frequency, i.e., $\omega_4 = 3\omega = \omega + \omega + \omega$, or the interaction involves one of the amplitudes taken with the reverse phase (or, formally, as a negative frequency $-\omega$), so $\omega_4 = \omega = \omega - \omega + \omega$. The former case is called third-harmonic generation (THG). The latter case is sometimes called self-action, and only introduces changes to the amplitude and phase of the existing electromagnetic field at ω. These changes are nevertheless of great practical significance, since they lead to effects such as self-focusing, soliton formation, all-optical switching, and nonlinear absorption processes such as two-photon absorption.

To extend the discussion of cubic optical nonlinearity from the molecular scale to the macroscopic (bulk) scale, one needs to consider the additivity of the individual molecular tensors and their respective orientation in space, as well as local field corrections. Dealing with hyperpolarizability tensors is greatly simplified when the nonlinear material under consideration is a collection of randomly oriented molecules, such as those in a liquid solution, or those in a solid solution, e.g., a molecularly-doped polymer, a polymer with nonlinear chromophores present as side groups, a sol–gel glass or ormosil containing chromophores, etc. Averaging of the γ_{ijkl} tensor over all orientations leads to an average $\langle\gamma\rangle$; for the case of a single electric field component acting on an assembly of nonlinear chromophores, $\langle\gamma\rangle$ is given by [12]:

$$\langle\gamma\rangle = \frac{1}{15}\gamma_{ijkl}(\delta_{ij}\delta_{kl} + \delta_{ik}\delta_{jl} + \delta_{il}\delta_{jk}), \tag{4}$$

where δ_{ij} is the substitution tensor (unity if $i = j$, zero otherwise). When the γ tensor is dominated by a single component γ_{1111}, this expression gives $\langle\gamma\rangle = 1/5\gamma_{1111}$. It should be noted that it is the average value of γ that is normally quoted as the measurement result when experiments are carried out on solutions of chromophores. The appropriate macroscopic measure of the cubic optical nonlinearity is the cubic nonlinear susceptibility $\chi^{(3)}(\omega_4;\omega_1,\omega_2,\omega_3)$, which can be defined

by macroscopic equations analogous to Eqs. (1) and (2) by considering the macroscopic analogue of the dipole moment, the polarization vector P, and its appropriate Fourier components. For a solution, the relation between $\chi^{(3)}$ and $\langle\gamma\rangle$ can be written as:

$$\chi^{(3)} = L^4 \sum_r N_r \langle\gamma\rangle_r, \tag{5}$$

where the index r extends over all components of the solution (the solvent as well as the solutes), N_r represents the concentration of a component molecule (in molecules cm^{-3}), and L is the local field correction factor, usually approximated by a Lorentz expression $L = (n^2+2)/3$, n being the refractive index. Similar to γ, $\chi^{(3)}$ is generally complex, i.e., it has real and imaginary parts:

$$\chi^{(3)} = \mathrm{Re}(\chi^{(3)}) + \mathrm{iIm}(\chi^{(3)}) = \chi^{(3)}_{\mathrm{real}} + \mathrm{i}\chi^{(3)}_{\mathrm{imag}}. \tag{6}$$

The third-harmonic generation (THG) process that is due to the cubic susceptibility $\chi^{(3)}(3\omega;\omega,\omega,\omega)$ is a general effect, i.e., it is exhibited by all matter, the contribution to THG from air being of particular importance in some experiments. Although THG may lead to up-conversion of laser beam frequency (e.g., from infrared at 1,064 nm to ultraviolet at 355 nm), the practical use of the process is difficult because of the near impossibility to equalize the velocity of the fundamental and third-harmonic waves in typical NLO materials. In practice, the third-harmonic of laser beams is obtained by a different route: doubling of frequency ω and then frequency summation of 2ω and ω in two subsequent quadratic NLO processes. However, THG is of importance, not only for testing of NLO properties of molecules, but also for laser diagnostics and for microscopic imaging of various objects including biological ones.

In contrast, the degenerate cubic NLO interaction, i.e., one in which the result of the interaction of three field components at ω is also at the same frequency ω, has numerous important applications. The notion that this interaction modifies amplitude and/or phase of the existing wave may be rephrased taking into account that the change in amplitude occurring at a certain distance is equivalent to absorption of light while the change in phase means slowing down or speeding up the wave, or, indeed, modification of the effective refractive index of the medium. Therefore, two practical effects of the degenerate cubic NLO interaction are described in terms of two simple quantities: the nonlinear refractive index n_2, defined by:

$$n(I) = n_0 + n_2 I \tag{7}$$

and the nonlinear absorption coefficient α_2, defined by:

$$\alpha(I) = \alpha_0 + \alpha_2 I, \tag{8}$$

where I represents the light intensity (related to the square of the electric field amplitude), and n_0 and α_0 are the refractive index and the absorption coefficient at

low light intensities, respectively. It can be shown that the nonlinear refractive index is related to the real part of $\chi^{(3)}$ by [13]:

$$n_2 = \frac{4\pi}{n_0 c} n_2' = \frac{12\pi^2}{n_0^2 c} \mathrm{Re}\left[\chi^{(3)}_{xxxx}(\omega;\omega,-\omega,\omega)\right]. \tag{9}$$

[Note that n_2' is a differently defined nonlinear index that relates the refractive index change to the square of the electric field amplitude]. The nonlinear absorption coefficient is related to the imaginary part of $\chi^{(3)}$ through [13]:

$$\alpha_2 = \frac{48\pi^3}{n_0^2 c\lambda} \mathrm{Im}\left(\chi^{(3)}_{xxxx}(\omega;\omega,-\omega,\omega)\right). \tag{10}$$

It is often convenient to treat the refractive index of a medium as a complex quantity $\hat{n} = n + \mathrm{i}k$, the real part of it being responsible for refraction and the imaginary part being responsible for absorption. Extending this to nonlinear phenomena, one can also treat the nonlinear index as complex and describe nonlinear refraction as being due to the real part of n_2 and nonlinear absorption as due to the imaginary part. An alternate way of expressing the nonlinear absorption properties of a molecule is by defining its nonlinear absorption cross-section. The two-photon absorption cross-section σ_2 is related to the imaginary part of γ of a molecule, and can be calculated from the nonlinear absorption coefficient α_2:

$$\sigma_2 = \frac{h\omega}{N}\alpha_2, \tag{11}$$

where N is the concentration of the absorbing molecules.

2.2 Experiment in Third-Order NLO Studies

Determination of cubic NLO properties of molecules is most often carried out in liquid solutions, but it is possible to use solid samples made by (for example) dispersing the chromophore in a host polymer, or as thin films of the pure compound under investigation, if the optical quality of the samples is sufficiently high. Depending on the method of measurement, the real and imaginary parts of $\chi^{(3)}$ (or n_2 and α_2) may be determined, but in some cases only the modulus $|\chi^{(3)}|$ is measured. The experimental techniques have been described in detail elsewhere [13], so only a short description of them is given here.

2.2.1 Third-Harmonic Generation

THG experiments remain popular for the estimation of cubic molecular nonlinearities. The experiment is usually carried out by recording the intensity of the third-harmonic generated by a beam from an infrared laser. Because of the many uncertainties related to the details of the generation of the third-harmonic, an often-adopted version of the experiment is carried out by recording fringes that appear when a thin film sample deposited on a glass plate is rotated out of the plane perpendicular to the laser beam. The resulting changes in the optical paths for the fundamental and third-harmonic beams lead to constructive or destructive interference. The fringe pattern thus obtained can be compared with one obtained for the glass plate alone, to evaluate both the amplitude and phase of $\chi^{(3)}(3\omega;\omega,\omega,\omega)$ for the thin film sample, which lead to the real and imaginary parts of $\chi^{(3)}$. A serious limitation of the THG technique when applied to organometallics is that $\chi^{(3)}(3\omega;\omega,\omega,\omega)$ may be quite different from $\chi^{(3)}(\omega;\omega,-\omega,\omega)$, which as discussed above has more practical significance – this is due to the fact that different resonances of the molecule contribute to these two susceptibilities (resonances close to ω and 3ω in the case of THG and resonances near ω and 2ω in the case of the degenerate susceptibility).

2.2.2 Z-Scan

Z-scan [14] (Fig. 1) is by far the most popular technique for investigations of the cubic molecular nonlinearities of organometallics, and is typically undertaken

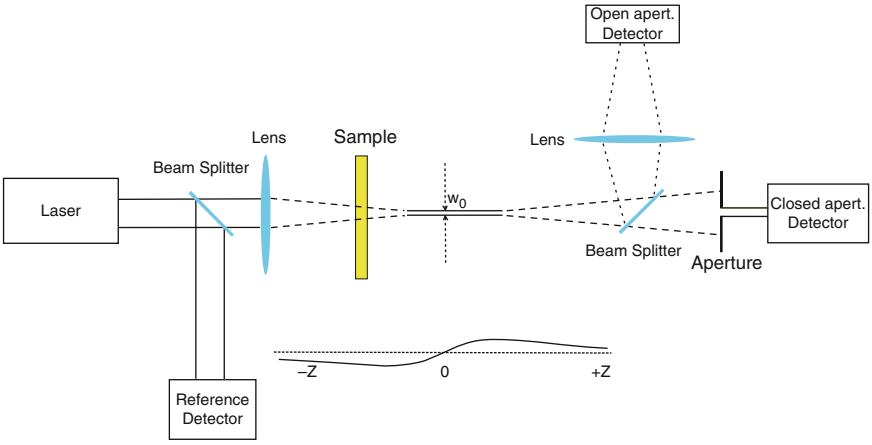

Fig. 1 Scheme of the *Z*-scan experiment in which the closed-aperture scan and the open-aperture scan are carried out simultaneously

with the organometallics in solutions of organic solvents. This ingenious technique consists in focusing a laser beam with a lens, scanning the sample to be investigated along the beam axis (the z-axis, hence the name Z-scan) in the range from a few Rayleigh lengths before the focal plane to a few Rayleigh lengths after the focal plane, and observing changes in the transmitted beam in the far field as a function of the position of the sample, z (the Rayleigh length is given by $z_R = \pi {w_0}^2/\lambda$, where w_0 is the laser beam spot size at focus). A very simple way of detecting distortion of the beam due to the self-focusing/self-defocusing effects imposed on it by the sample is by placing a small aperture in the far field and recording the power transmitted through this aperture as a function of z. The sample starts its travel at the point where the beam is still relatively large and therefore the light intensity is low, but as it comes closer to the focal plane at $z = 0$, the intensity increases and is then reduced again. These intensity variations lead to formation in the sample of an induced positive (self-focusing, $n_2 > 0$) or negative (self-defocusing, $n_2 < 0$) lens whose effect is to add to that of the primary lens and to modify the shape of the beam in the far field. As the beam becomes larger or smaller through focusing/defocusing, the aperture transmittance increases or decreases, and these variations (in the so-called closed-aperture scan) can be compared to those predicted from a theoretical computation.

While self-focusing and self-defocusing are manifestations of the refractive part of the degenerate cubic optical nonlinearity, the absorptive part results in variation of the total power of the beam transmitted through the sample as a function of z. This can be monitored with a detector that integrates the power in the whole beam, and the changes of such power as a function of z (in the so-called open-aperture scan) can be directly related to the nonlinear absorption coefficient of the sample, α_2.

2.2.3 Nonlinear Absorption and Nonlinear Absorption-Induced Fluorescence

Open-aperture Z-scan is often used to measure nonlinear absorption alone, particularly in cases where such absorption is more complicated than a simple two-photon process. Alternatively, one can simply measure the transmittance of a sample as a function of the incident laser power (by attenuation of the laser beam, without changing its focusing), and then deduce the nonlinear absorption parameters from the deviation from linearity of the transmission vs power plot. A very convenient method of measuring two-photon absorption cross-section is where the degree of nonlinear absorption is judged from the amount of two-photon-induced fluorescence emitted by a sample exposed to short laser pulses in a wavelength range where there is no one-photon absorption. This popular technique is, however, seldom applicable to organometallics, for which fluorescence is commonly strongly quenched by the metal atoms.

2.2.4 Degenerate Four-Wave Mixing and Pump-Probe Measurements

One of the crucial problems in the determination of cubic optical nonlinearity parameters is whether the effects measured are really due to the electronic hyperpolarizabilities of molecules, or if they are a result of more complicated NLO processes which may involve such effects as multistep multiphoton absorption (i.e., one-photon absorption followed by excited-state absorption), nonlinear refraction due to the presence of short or long-lived excitation, or even thermal effects due to the deposition of heat by linear and nonlinear absorption processes occurring in the sample under investigation. The *Z*-scan technique is not suitable for resolving issues of this kind (although it is often assumed that the use of low repetition rate femtosecond laser pulses minimizes the contribution of the unwanted cumulative effects). Time-resolved techniques can be employed instead. The principle of these techniques is that a beam (or a pair of beams) carrying short (femtosecond or picosecond) laser pulses is directed onto a sample and produces a transient change in the optical properties of the sample, i.e., it changes either its refractive (refractive index) or absorptive properties. In the case of degenerate four-wave mixing (DFWM), the two beams used as the pump interfere in the sample, and actually create a volume grating of the absorptive and/or refractive properties modification. A probe beam is directed at the sample after a delay, the delay being produced by passing the probe beam through a slightly longer path than that of the pump beam(s). The effect on the probe beam is that its transmission may vary depending on the degree of the change induced in the sample, or it may be diffracted to a certain degree, both depending on the strength of the existing induced grating in the sample. The measurements of these changes in the probe beam or the diffracted beam, as a function of the delay of the pump compared to the probe, allow one to estimate the magnitude of the nonlinear effects and to evaluate their temporal evolution, and thereby allow one to conclude whether the effects are essentially instantaneous or if they are due to processes having a certain lifetime.

3 Structure-Property Developments Since 2000

There has been considerable activity in correlating structural changes to the magnitude of optical nonlinearities for various types of organometallics in the past few years, but ferrocene complexes and metal alkynyl complexes continue to be the most intensively studied classes of organometallics in NLO. While earlier studies focused on simple compounds coupling ferrocenyl groups to organic π-delocalizable groups, ferrocenyl units have now been used to construct organometallic-coordination hybrid complexes such as **1** [15]. *Z*-scan studies at 532 nm using 8 ns pulses for **1**, the ferrocenyl ligand, and related mercury- and cadmium-containing derivatives suggest that the nonlinearity derives from the ferrocenyl ligand and

that there is little contribution from the posttransition metal. The reported γ values are five to six orders of magnitude larger than previously reported data for ferrocenyl complexes obtained with femtosecond pulses, so there are likely to be contributions from thermal effects, photochemical changes, and other cumulative effects, particularly excited-state absorption.

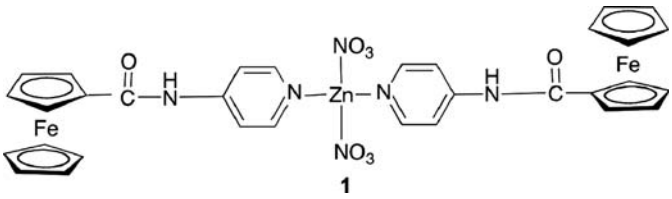

1

Most of the earlier studies of ruthenium alkynyl complexes bearing acceptor substituents involved 4-nitrophenyl groups on the alkynyl ligand. This has now been extended to complexes **2**–**4** bearing barbiturate acceptor groups, which were assessed by DFWM at 532 nm using picosecond pulses [16]. As is the case with 4-nitro-containing complexes, nonlinearity increases on π-bridge lengthening, with complex **4** the most active of the complexes examined.

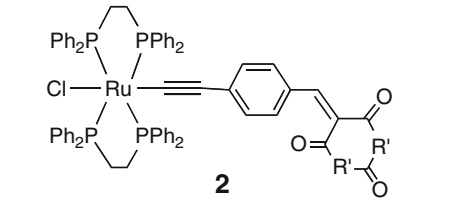

2

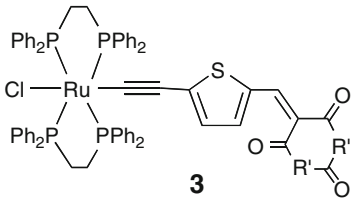

3

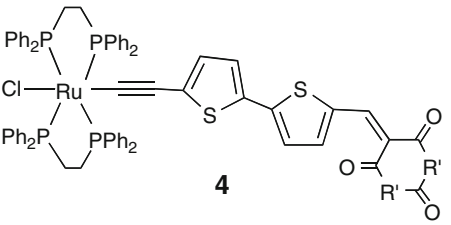

4

R' = NH, NMe

There has been enormous interest in the optical limiting properties of transition metal clusters in the past decade. Most data result from *Z*-scan studies with ns pulses at 532 nm. For example, the half-open cubane-like clusters $WCu_3(\mu_3\text{-}S)_3(\mu\text{-}Br)Br(EPh_3)_2(\eta^5\text{-}C_5Me_5)$ (E = P, As (**5**)) show similar threshold limiting values, with the phosphine-containing cluster revealing somewhat greater nonlinear absorption at the same concentration [17]. The cyclic complex $(\eta^5\text{-}C_5Me_5)(S)W\{(\mu\text{-}S)Au(\mu\text{-}S)_2W(\eta^5\text{-}C_5Me_5)(\mu\text{-}S)\}Au(\mu\text{-}S)$ (**6**) in which the metal atoms are held together solely by bridging sulfido ligands was examined by a combination of ps DFWM and ns *Z*-scan studies [18]. While the reported nonlinearities are large, these data were collected at 532 nm, a wavelength that corresponds to moderate linear absorption

for this compound and indeed most of the clusters to have been examined thus far. Studies of clusters over a broad wavelength range are lacking. Since the optical limiting phenomenon occurring in the nanosecond domain is most often due to a combination of processes, involving among others one-photon absorption, two-photon absorption, and excited state absorption, the lack of wide wavelength and time-resolved studies restricts the possibilities of any generalization of the results or, in fact, correlation between the structural features of the investigated molecules, their photophysical properties, and the power limiting merit.

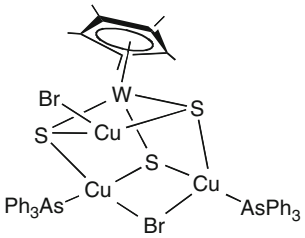

5

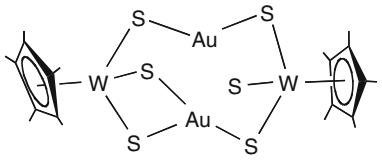

6

4 Spectral Dependencies

The vast majority of reports of the third-order NLO properties of organometallics have focused on results from a single laser irradiation wavelength. These data are most useful when comparing efficiency for specific applications at that wavelength. The problem with this approach is that contrasting data obtained for a range of complexes at a single wavelength rarely affords a structure-property outcome similar to that obtained from a comparison of the maximal values from a wide-spectral range study. Difficulty in access to wide-spectral range NLO data has retarded the development of this area. Almost all of the spectral dependencies as currently exist for organometallics have been obtained from a tedious point-by-point data collection using the *Z*-scan technique and a tunable light source. The recently-developed techniques of white-light continuum *Z*-scan and white-light continuum pump-probe have been applied to organic molecules [19–24], inorganic complexes [25–27], inorganic semiconductors [28, 29], and organic polymers [30, 31], but the only application to organometallics thus far is to (η^5-cyclopentadienyl)(η^6-cumene)iron (III) hexafluorophosphate (Irgacure 261), a commercially-available photo-initiator, whose maximal 2PA cross-section was found to be very low and could only be defined in terms of an upper bound (<20 GM) [20]. It can confidently be anticipated that application of this new technique to organometallics will expand in the future.

Thus far, there has only been one study of a systematically-varied series of organometallic complexes. Femtosecond *Z*-scan measurements of the platinum-terminated polyynes *trans,trans*-{(*p*-$MeC_6H_4)_3P\}_2$(*p*-MeC_6H_4)Pt($C{\equiv}C)_n$Pt(*p*-C_6H_4Me){P(*p*-$C_6H_4Me)_3\}_2$ (**7**) (n = 3–6, 8, 10, 12) afforded two-photon absorption maxima that were shown to red-shift upon chain lengthening [32].

Extrapolation of the sp-carbon chain length dependence of nonlinear absorption maxima permitted an estimate (neglecting saturation) of 1,000 nm for that of the infinite carbon chain, carbyne. The maximal values increase superlinearly on chain lengthening, and can be fitted to a power law with an exponent of ca. 1.8, suggesting that longer chain examples than are currently experimentally accessible will have extraordinarily large σ_2 values.

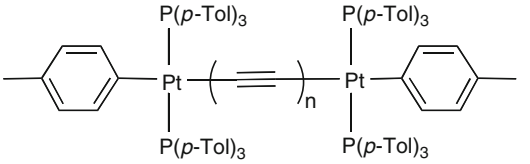

7

n = 3-6, 8, 10, 12

Two similar alkynylruthenium dendrimers with nitro groups at the periphery have been shown to have very different nonlinear absorption behavior. Dendrimer **8**, which possesses ligated ruthenium units at the outermost branches only, revealed dispersion of the cubic nonlinearity that could be modeled by simple relations assuming competition between two-photon absorption and absorption saturation [33]. Dendrimer **9** has ligated ruthenium groups at both the core and periphery of the dendrimer. While the short wavelength behavior (625–950 nm) corresponds to a two-photon absorption process, the longer wavelength profile (1,000–1,300 nm) is consistent with the dominance of three-photon absorption, and the dendrimer possesses a record 3PA coefficient [34]. The advantages that accrue from exploiting

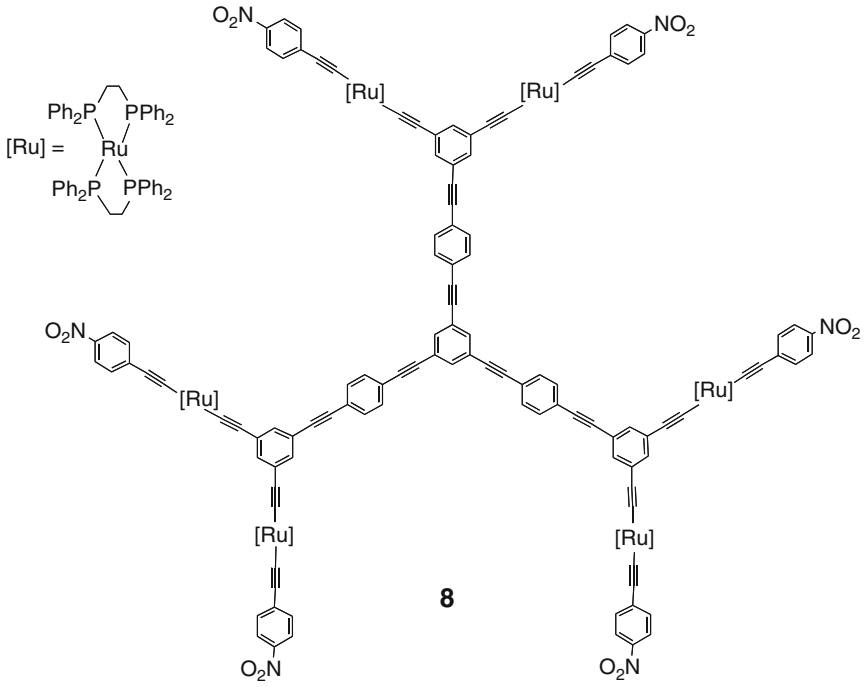

8

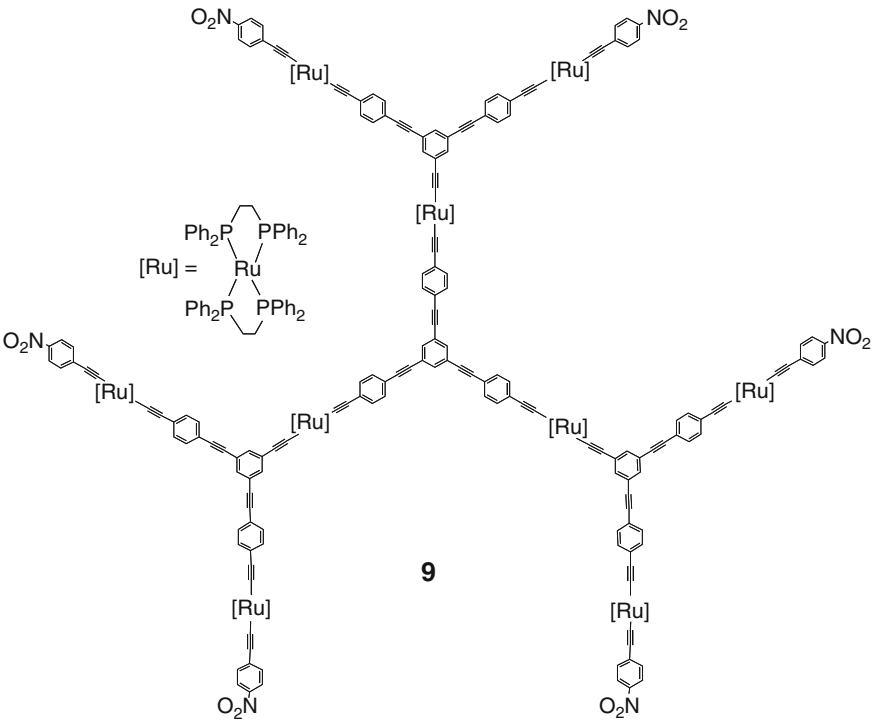

multiphoton processes (superior resolution for applications requiring spatial control, and the opportunity to use longer and therefore technologically-desirable wavelengths) are accentuated when proceeding from two-photon absorption to three-photon absorption, but little is known of how to optimize the 3PA coefficient. This field is still in its infancy – it is to be hoped that further reports of such fifth-order (quintic) nonlinearity are forthcoming for organometallics in the near future.

5 Switching

The magnitudes of optical nonlinearities of organometallics approach those of the best organics, but to justify the possible additional costs associated with organometallics (such as potentially expensive metals and ligands, less stable compounds, lower-yielding and longer synthetic procedures) necessitates "value-adding" to what is possible with purely organic compounds. One area in which organometallics may be superior to organics is modulating or switching nonlinearity. The most popular approaches to reversible switching of molecular NLO properties are by protonation/deprotonation, oxidation/reduction, or photoisomerization procedures [35]. Of these three approaches, the ready accessibility of metals in multiple stable oxidation states suggests that redox switching of optical nonlinearity may be an area

in which organometallics are preferred. The cubic nonlinearities of several ruthenium alkynyl complexes and dendrimers have been switched in situ in a modified optically-transparent thin-layer electrochemical (OTTLE) cell [36–39], with several examples corresponding to reversing the sign and magnitude of nonlinear refraction and nonlinear absorption, and a specific example corresponding to a cubic NLO "on/off" switch. Incorporation of metals with widely differing oxidation potentials into the one NLO-active molecule affords the prospect of multiple NLO states. Applying an appropriate potential to the heterobimetallic complex **10** allows one to access the Fe^{II}/Ru^{II}, Fe^{III}/Ru^{II}, and Fe^{III}/Ru^{III} states, all of which have distinct linear optical and NLO properties; at 790 nm, open-aperture *Z*-scan studies reveal that the Fe^{II}/Ru^{II}, Fe^{III}/Ru^{II}, and Fe^{III}/Ru^{III} states correspond to effectively zero nonlinear absorption, two-photon absorption, and saturable absorption, respectively, or zero, positive, and negative values of the imaginary component of the cubic nonlinearity [40].

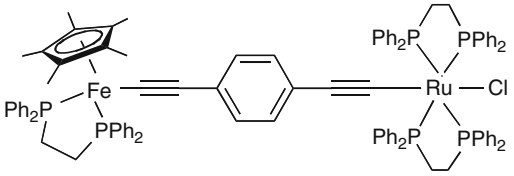

10

Switching the cubic nonlinearity of ruthenium alkynyl complexes by a protonation/deprotonation sequence (via a vinylidene complex) was demonstrated by fs *Z*-scan studies at 800 nm several years ago [41]. Recently, protic and electrochemical switching were demonstrated in the ruthenium alkynyl cruciform complex **11** for which distinct linear optical and NLO behavior were noted for the vinylidene complex and the Ru(II) and Ru(III) alkynyl complexes [42]. Because the oxidation/reduction and protonation/deprotonation procedures are independent, this system corresponds to switching by "orthogonal" stimuli.

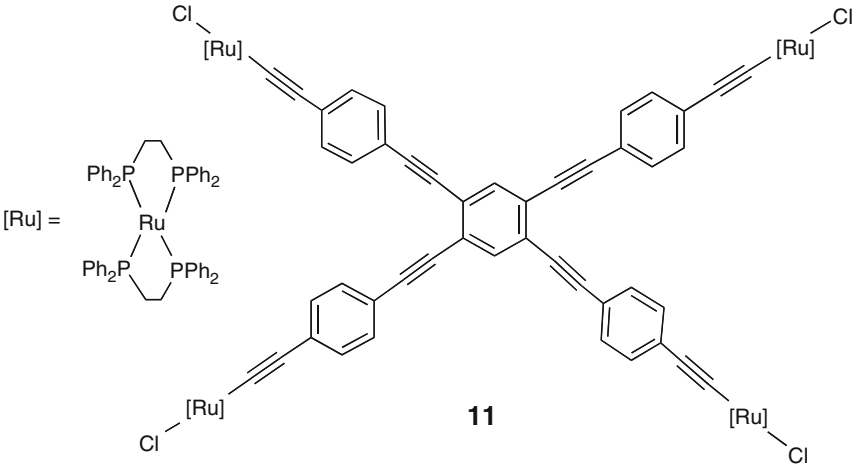

11

6 Materials

The major focus of third-order NLO studies with organometallics over the past few years has continued to be solution measurements, which permit assessment of molecular nonlinearities and development of structure-property relationships; reports of bulk susceptibilities of organometallic-containing films are comparatively rarer. Bis(arene)chromium complexes have been incorporated into cyano-containing polymeric matrices and very high purely electronic third-order NLO susceptibilities of the resultant polymeric films have been noted from *Z*-scan and spectrally-resolved two-beam coupling studies [43]. The molar ratio of Cr:monomer was as high as 1:4, and the resultant homogeneous oligomeric product, which is produced by cyanoethylation of the metal-bound arene rings, was assessed as containing ca. eight monomer units. The *Z*-scan studies (utilizing 40 ps pulses at 1,064 nm or 3 ps pulses at 1,054 nm) afforded $\chi^{(3)}$ values as high as -1.7×10^{-10} esu, of the same order as the best organic polymer materials. Spectrally-resolved two-beam coupling using fs pulses and a central wavelength of 795–800 nm confirmed that the test composites exhibit significant ultrafast electronic nonlinearity.

The alkynylruthenium complexes **12**–**14** were spin-coated from dichloromethane solution and the resultant ca. 0.2 μm thick films assessed by THG using 15 ps pulses at 1,064 nm, with a ca. 50% increase in $\chi^{(3)}$ value noted on proceeding from **12** to **13** and **14** consistent with an extended π-system for the latter complexes involving the *trans*-disposed alkynyl ligands [44].

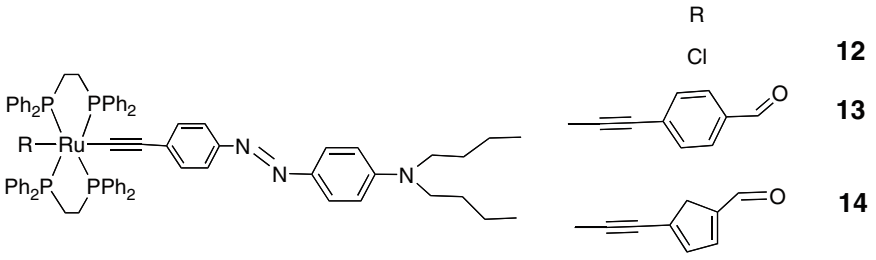

7 Conclusion

In contrast to the rapid development of structure–property relationships for quadratic optical nonlinearities of organometallics, the effect of molecular variation on cubic NLO properties has been slow to be systematized, a shortcoming that access to broad-wavelength-range fs sources should progressively address. While initial emphasis with organometallics was in using the metal center to stabilize reactive organics and afford unusual geometries and thereby charge distributions, recent studies have focused on exploiting access to multiple stable oxidation states, thereby affording access to new types of molecular NLO switches.

Materials development exploiting cubic NLO properties of organometallics has been slow, reflecting the fact that the focus is still on molecular rather than bulk material properties. It is to be hoped, however, that future studies will involve the organometallics with the most promising molecular NLO properties and will attempt to use these to meet the NLO material challenges of nanophotonics and biophotonics, e.g., the need for highly efficient nonlinear absorbers for use in nanofabrication, 3D memories, and bioimaging.

References

1. Marder SR, Sohn JE, Stucky GD (1991) Materials for nonlinear optics, chemical perspectives. ACS, Washington DC
2. Marder SR (1992) In: Bruce DW, O'Hare D (eds) Inorganic materials. Wiley, Chichester, UK
3. Long NJ (1995) Angew Chem Int Ed Engl 34:21–38
4. Whittall IR, McDonagh AM, Humphrey MG, Samoc M (1999) Adv Organomet Chem 43: 349–405
5. Gray GM, Lawson CM (1999) In: Roundhill DM, Fackler JP Jr (eds) Optoelectronic properties of inorganic compounds. Plenum, New York, NY
6. Kershaw SV (1999) In: Roundhill DM, Fackler JP Jr (eds) Optoelectronic properties of inorganic compounds. Plenum, New York, NY
7. Long NJ (1999) In: Roundhill DM, Fackler JP Jr (eds) Optoelectronic properties of inorganic compounds. Plenum, New York, NY
8. Morrall JP, Dalton GT, Humphrey MG, Samoc M (2008) Adv Organomet Chem 55:61–136
9. Roy S, Kulshrestha K (2005) Opt Commun 252:275–285
10. Liu Y-C, Kan Y-H, Wu S-X, Yang G-C, Zhao L, Zhang M, Guan W, Su Z-M (2008) J Phys Chem A 112:8086–8092
11. Shi RF, Garito AF (1998) In: Kuzyk MG, Dirk AF (eds) Characterization techniques and tabulations for organic nonlinear optical materials. CRC, Boca Raton, USA
12. Buckingham AD, Pople JA (1955) Proc Phys Soc A 68:905–909
13. Sutherland RL (2003) Handbook of nonlinear optics, 2nd edn. Marcel Dekker, New York
14. Sheikh-bahae M, Said AA, Wei T, Hagan DJ, Van Stryland EW (1990) IEEE J Quantum Electron 26:760–769
15. Li G, Song Y, Hou H, Li L, Fan Y, Zhu Y, Meng X, Mi L (2003) Inorg Chem 42:913–920
16. Luc J, Migalska-Zalas A, Tkaczyk S, Andriès J, Fillaut J-L, Meghea A, Sahraoui B (2008) J Optoelectron Adv Mater 10:29–43
17. Lang J-P, Sun Z-R, Xu Q-F, Yu H, Tatsumi K (2003) Mater Chem Phys 82:493–498
18. Lang J-P, Yu H, Ji S-J, Sun Z-R (2003) Phys Chem Chem Phys 5:5127–5132
19. De Boni L, Andrade AA, Misoguti L, Mendonça CR, Zilio SC (2004) Opt Express 12: 3921–3927
20. Schafer KJ, Hales JM, Balu M, Belfield KD, Van Stryland EW, Hagan DJ (2004) J Photochem Photobiol A Chem 162:497–502
21. Collini E, Ferrante C, Bozio R (2005) J Phys Chem B 109:2–5
22. Lepkowicz RS, Cirloganu CM, Fu J, Przhonska OV, Hagan DJ, Van Stryland EW, Bondar MV, Slominsky YL, Kachkovski AD (2005) J Opt Soc Am B 22:2664–2685
23. Zheng S, Leclercq A, Fu J, Beverina L, Padilha LA, Zojer E, Schmidt K, Barlow S, Luo J, Jiang S-H, Jen AK-Y, Yi Y, Shuai Z, Van Stryland EW, Hagan DJ, Brédas J-L, Marder SR (2007) Chem Mater 19:432–442
24. Signorini R, Ferrante C, Pedron D, Zerbetto M, Cecchetto E, Slaviero M, Fortunati I, Collini E, Bozio R, Abbotto A, Beverina L, Pagani GA (2008) J Phys Chem A 112:4224–4234

25. De Boni L, Gaffo L, Misoguti L, Mendonça CR (2006) Chem Phys Lett 419:417–420
26. De Boni L, Correa DS, Pavinatto FJ, dos Santos DS Jr, Mendonça CR (2007) J Chem Phys 126:165102-1–165102-4
27. De Boni L, Piovesan E, Gaffo L, Mendonça CR (2008) J Phys Chem A 112:6803–6807
28. Balu M, Hales J, Hagan DJ, Van Stryland EW (2004) Opt Express 12:3820–3826
29. Balu M, Hales J, Hagan DJ, Van Stryland EW (2005) Opt Express 13:3594–3599
30. Oliveira SL, Corrêa DS, De Boni L, Misoguti L, Zilio SC, Mendonça CR (2006) Appl Phys Lett 88:021911-1–021911-3
31. Corrêa DS, De Boni L, Gonçalves VC, Balogh DT, Mendonça CR (2007) Polymer 48:5303–5307
32. Samoc M, Dalton GT, Gladysz JA, Zheng Q, Velkov Y, Ågren H, Norman P, Humphrey MG (2008) Inorg Chem 47:9946–9957
33. Powell CE, Morrall JP, Ward SA, Cifuentes MP, Notaras EGA, Samoc M, Humphrey MG (2004) J Am Chem Soc 126:12234–12235
34. Samoc M, Morrall JP, Dalton GT, Cifuentes MP, Humphrey MG (2007) Angew Chem Int Ed 46:731–733
35. Coe BJ (1999) Chem Eur J 5:2464–2471
36. Cifuentes MP, Powell CE, Humphrey MG, Heath GA, Samoc M, Luther-Davies B (2001) J Phys Chem A 105:9625–9627
37. Powell CE, Cifuentes MP, Morrall JPL, Stranger R, Humphrey MG, Samoc M, Luther-Davies B, Heath GA (2003) J Am Chem Soc 125:602–610
38. Powell CE, Humphrey MG, Cifuentes MP, Morrall JP, Samoc M, Luther-Davies B (2003) J Phys Chem A 107:11264–11266
39. Cifuentes MP, Powell CE, Morrall JP, McDonagh AM, Lucas NT, Humphrey MG, Samoc M, Houbrechts S, Asselberghs I, Clays K, Persoons A, Isoshima I (2006) J Am Chem Soc 128:10819–10832
40. Samoc M, Gauthier N, Cifuentes MP, Paul F, Lapinte C, Humphrey MG (2006) Angew Chem Int Ed 45:7376–7379
41. Hurst SK, Cifuentes MP, Morrall JPL, Lucas NT, Whittall IR, Humphrey MG, Asselberghs I, Persoons A, Samoc M, Luther-Davies B, Willis AC (2001) Organometallics 20:4664–4675
42. Dalton GT, Cifuentes MP, Petrie S, Stranger R, Humphrey MG, Samoc M (2007) J Am Chem Soc 129:11882–11883
43. Klapshina LG, Grigoryev IS, Lopatina TI, Semenov VV, Domrachev GA, Douglas WE, Bushuk BA, Bushuk SB, Lukianov AYu, Afanas'ev AV, Benfield RE, Korytin AI (2006) New J Chem 30:615–628
44. Luc J, Niziol J, Niechowski M, Sahraoui B, Fillaut J-L, Krupka O (2008) Mol Cryst Liq Cryst 485:990–1001